Experimental determination of shielding factor for a Swedish farmhouse

Mikael Westin

LUND UNIVERSITY

Bachelor Thesis
January 2014

Department of Medical Radiation Physics, Malmö
Lund University, Sweden

Supervisor: Christian Bernhardsson, PhD

Abstract

The protection that different types of buildings can provide against gamma radiation from radioactive fallout has been investigated since the late 1950s. The DCPA Standard Method has served as the basis to determine this protection, which is given by the so called "protection factor". Several studies in the U.S. have utilized enclosed sources of radioactive nuclides to simulate fallout and test the Standard Method. Following the Chernobyl accident a set of measurements were performed in the Gävle region of Sweden to determine the protection that typical Swedish dwellings would provide against fallout gamma. The determined protection was quantized in the so called "Shielding factor", a quantity similar to the protection factor.

In recent years, a need has emerged for a feasible method to experimentally determine the protection that buildings may provide against fallout radiation. In this paper the possibility of determining the shielding factor with the help of *in situ* gamma spectrometry and point sources has been investigated. The aim of the study was to see whether the *in situ* spectrometric method of determining shielding factors would be possible to perform with point sources for a given building and, if so, the determined shielding factor would be similar to earlier determined values.

A building, and associated land, was lent from the Swedish Armed Forces. An enclosed source of ^{137}Cs was placed according to a predetermined pattern around the building and the resulting count rate was registered by a 123% HPGe detector positioned inside the building. With the obtained spectrum data, measured dimensions of the house and a calculated buildup factor, the shielding factor for the building could be assessed.

The shielding factor for the farmhouse was estimated to be in the range of 0.093-0.10. Furthermore, the measurements were carried out within the planned time frame and without exposing the personnel to dose levels above guideline values.

The *in situ* spectrometric method of determining shielding factors in combination with point sources seems promising. However, in order to fully assess whether or not the method can be used to determine the shielding factor for a given house further investigations are needed in order to establish the precision of the method and the uncertainties that the method imposes on the shielding factor.

Table of contents

1 Introduction

From the late 1950s until the mid-1970s, the United States put a lot of effort into determining the protection that different types of buildings could provide against radiation from nuclear fallout. Under the supervision of the Defense Civil Preparedness Agency[1] (DCPA) the so called "*DCPA Standard Method for Fallout Gamma Radiation Shielding Analysis*[2]" was developed (DCPA, 1976). Major contributions to the theoretical basis of the Standard Method was performed by Spencer (1962) and practical implementations of the method have been described in several papers (*e.g.* OCDM, 1961; Eisenhauer, 1964). Various aspects of the Standard Method have been tested experimentally in a number of different experiments during the late 1950s and the early 1970s. Many of the experiments performed have included a large number of gamma emitting point sources to simulate nuclear fallout, *e.g.*, Auxier *et al.* (1959) used four hundred 154 MBq sources of ^{60}Co, positioned on a metal grid, to investigate the shielding properties of structures resembling typical North American residences. However, the experiments of Auxier *et al.* were limited to a restricted number of sites due to the large amount of activity that was used. Another experiment, focusing on the shielding of structures against gamma radiation from both ground and roof deposited fallout, was performed by Burson *et al.* (1969). In this test fallout was simulated by a large number of ^{60}Co sources that were hydraulically pumped through tubes placed in various patterns around different military buildings in the Nevada desert. The results from the experiments conducted by Burson *et al.* were estimated to agree within ±25% to ±50% (depending on the type of structure) with the values predicted by the Standard Method. The procedures presented in the Standard Method have served as the basis for several countries, besides the U.S., in regard to assess the shielding that structures may provide. Apart from the limited number of *in situ* measurements, different types of computer programs incorporating elements of the Standard Method have been developed. Notably, the computer program KVAST[3] developed by Elvers *et al.* (1979) at the Swedish Defense Research Establishment[4] (FOA) has the Standard Method as a basis for determining the protection afforded by structures (Finck, 1992)

In recent years, a need has emerged[5] for a feasible method to experimentally determine the protection that buildings may provide against fallout radiation. Although the Standard Method can provide a detailed and comprehensive assessment of the shielding properties of a structure it has been shown that practical trials of the Standard Method require substantial technical resources and funding. Thus, the need for an updated, rapid and less expensive method is obvious. The development of high resolution gamma spectrometry has provided new methods of assessing the shielding that houses can provide. Following the Chernobyl accident the so called *in situ* spectrometric method for assessing the protection provided by houses was devised by Finck (1992). Although not identical to the Standard Method, the *in situ* spectrometric method may be applied to assess the shielding factor that a house will provide.

In the following paper the prospect of using a simplified version of the *in situ* spectrometric method, for a specific house, has been investigated. Comparison with theoretical calculations is also carried out in in order to assess the feasibility of the simplified method.

[1] The DCPA no longer exists as a separate department. The assignments that the DCPA had is at present time (2013) managed by the United States Department of Homeland Security (USDHS).
[2] Henceforth referred to as the "*Standard Method*".
[3] *KVArvarande STrålning*: KVAST.
[4] The FOA no longer exists as a separate department. By merging with the Swedish Institute for Aeronautic Research (FFA) the Swedish Defense Research Agency (FOI) was created in 2001. At present time FOI handles the assignments that FOA formerly had.
[5] The following report is part of the work to develop new methods of determining shielding factors *(SSM research grant*, SSM2013-1545).

2 The shielding factor

As pointed out by Finck (1992), several terms have been used in the literature to denote the shielding that structures may offer against external radiation from ground deposited fallout. In accordance with the work of Finck, the term "*shielding factor*" is adopted in this paper to indicate the protection effect that structures may offer against gamma radiation from ground deposited fallout. A brief introduction to the shielding factor follows below.

2.1 Definition of the shielding factor

Following a severe reactor accident or an atmospheric detonation of a nuclear weapon, several sources of exposure will emerge:

i.	Irradiation from radioactive cloud	(external irradiation);
ii.	Irradiation from deposited radioactive material	(external irradiation);
iii.	Irradiation from inhaled radionuclides	(internal irradiation);
iv.	Irradiation from ingested radionuclides	(internal irradiation).

Buildings can offer various degree of protection against i.-iii., depending on design (size, shape and material). The Standard Method can account for reduction in exposure due to i. and ii. In the Standard Method, the degree of protection that a structure may offer at a specific location is related to the exposure at the same unshielded location to yield a quantitative term called the "*Reduction Factor*" (RF) (DCPA, 1976). To better understand the reduction factor the kerma rate $(\dot{K})$, at a specific point, may be considered. The kerma rate can be written as:

$$\dot{K} = \int_{E=0}^{E_{max}} \dot{\psi}(E) \left(\frac{\mu_{tr}}{\rho}\right)_{E,Z} dE, \tag{1}$$

where $\dot{\psi}(E)$ *is* the differential distribution of photon energy fluence and $(\mu_{tr}/\rho)_{E,Z}$ is the mass energy-transfer coefficient (Attix, 2004). Ideally, if the detector registers all photon energies with 100% efficiency over all spherical directions[6], when placed 3 feet above an infinite plane source the detector will register a kerma rate equal to $(\dot{K}_{ref})$. If a building (for simplicity, a box-shaped building is considered) is placed around the detector and the surface area, corresponding to the building floor, is cleared of radioactive particles the detector will register a kerma rate equal to $(\dot{K}_{bld})$. The reduction factor can now be defined as the quotient between the measurement in the house and the measurement above the unshielded, infinite plane source, *i.e.*

$$RF = \frac{\dot{K}_{bld}}{\dot{K}_{ref}}. \tag{2}$$

Provided that charged-particle equilibrium is present (*i.e.*, the kerma rate may be taken as the dose rate), Eq. (2) is consistent with the original definition of the reduction factor[7] (Spencer, 1962). In this paper the shielding factor *(S_{bld})* is equated with the reduction factor, *i.e.*

$$S_{bld} \equiv RF = \frac{\dot{K}_{bld}}{\dot{K}_{ref}}. \tag{3}$$

[6] Such a detector does not exist, but this is not of any consequence in the following description of the RF. For more information about gamma-detectors see, *e.g.*, Leo (1994).

[7] Sometimes the term "*protection factor*" (PF) is used. Whether one uses the PF or the RF to denote the protection effect of houses is usually not a problem, since the reciprocal of one yields the other. However, the distinction between the two terms is worth to mention since they may easily be confused. The protection factor is defined as the reciprocal to the reduction factor (Spencer, 1962).

However, the definition in Eq. (3) is difficult to use in practice since it requires measurements of the kerma rate above an infinite plane source. This problem can be avoided by introducing the so called "*ground roughness shielding factor*":

$$S_{gnd} = \frac{\dot{K}_{gnd}}{\dot{K}_{ref}}. \tag{4}$$

The numerator in Eq. (4) is the kerma rate measured one meter above a fallout source having the same deposition density as the infinite plane source. Ground roughness shielding factors between 0.5-1.0 have been reported in the literature (Finck, 1992) and the subject has been thoroughly investigated in the report by Huddleston *et al.* (1965). Combining equations (3) and (4) yields

$$S_{bld} = S_{gnd} \frac{\dot{K}_{bld}}{\dot{K}_{gnd}}. \tag{5}$$

Now, if the ground surrounding a building is flat and has few shielding obstacles between the building and the gamma-sources, (S_{gnd}) will approach unity, *i.e.*, the shielding factor can be approximated by

$$S_{bld} \approx \frac{\dot{K}_{bld}}{\dot{K}_{gnd}}. \tag{6}$$

Using this definition the shielding factor is always $0 \leq S_{bld} \leq 1$, with maximum shielding for $S_{bld} = 0$. By carefully choosing the measuring site and by using point sources located on top of the ground the requirements of negligible ground roughness can be met. Still, it should be pointed out that Eq. (6) generally overestimates[8] the shielding factor and that a real fallout will have a depth distribution down in the soil that will, in part, attenuate the fallout gamma radiation and alter the spectral distribution with height above the ground (Huddleston *et al.*, 1965).

2.2 Measuring the shielding factor –The total gamma method

A straightforward way of experimentally determining the shielding factor for a house may be done by the so called "*total gamma method*" (Finck, 1992). Provided that ground roughness is negligible (*i.e.* Eq. (6) is valid) the shielding factor can be determined by measuring the kerma rate in four steps, as illustrated in Fig. 1.

[8] This, however, will yield a conservative value of the shielding factor which, from a radiation protection perspective, may be more eligible than the reverse situation of underestimating the shielding factor.

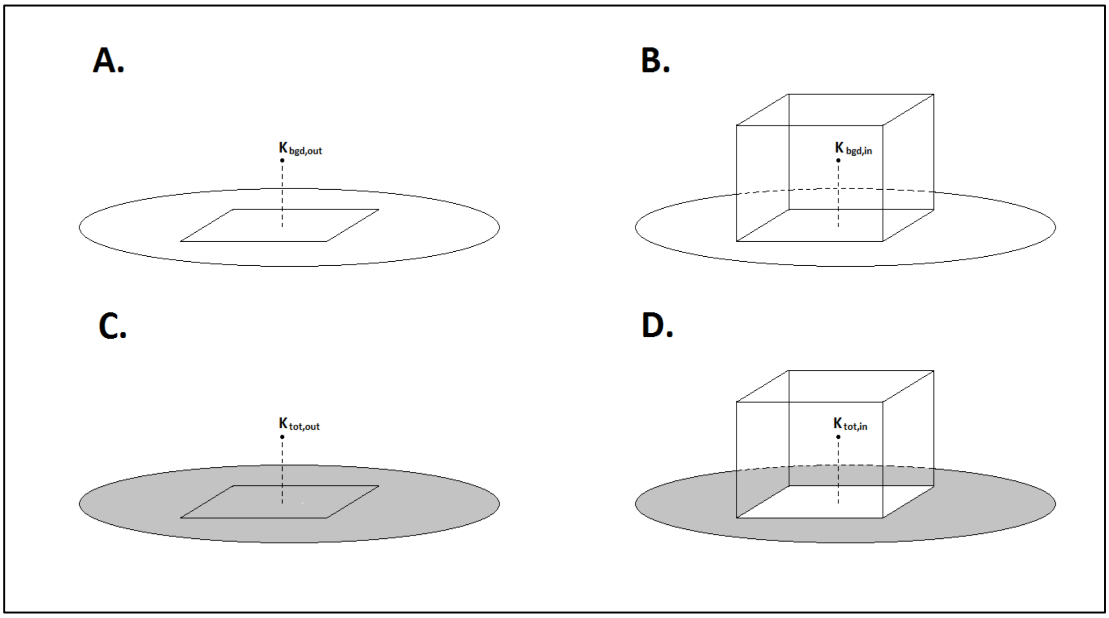

Figure 1: Schematic illustration of how the shielding factor can be obtained from measuring the kerma rate under four different situations (**A**-**D**). **A**: Kerma rate outside the building with no artificial activity present ($\dot{K}_{bgd,out}$). **B**: Kerma rate inside the building with no artificial activity present ($\dot{K}_{bgd,in}$) **C**: Kerma rate outside with artificial activity present ($\dot{K}_{tot,out}$). **D**: Kerma rate inside the building with artificial activity present ($\dot{K}_{tot,in}$).

Following the measuring procedure illustrated in Fig. 1 the shielding factor may be calculated according to:

$$S_{bld} = \frac{\dot{K}_{tot,in} - \dot{K}_{bgd,in}}{\dot{K}_{tot,out} - \dot{K}_{bgd,out}}. \tag{7}$$

The disadvantage of using the total gamma method in connection with real fallout (*e.g.* from the Chernobyl accident) is that the kerma rate due to background radiation before the building was constructed is usually unknown. However, the total gamma method illustrates in a clear way how the shielding factor of a building can be quantified in terms of kerma rates.

2.3 Measuring the shielding factor – The *in situ* spectrometric method

Another way of determining shielding factors for buildings is by a modification of the method of *in situ* high resolution gamma spectrometry[9]. The method of determining shielding factors by *in situ* measurements has been described by Finck (1992). The following paragraph (2.3.1-2.3.2) presents the main features of that method.

2.3.1 The shielding factor for primary fluence

The shielding factor for primary radiation ($S_{p,bld}(E)$) can be defined in a similar way as the shielding factor (Eq. (3)), but with the kerma rates replaced by the corresponding quantities due to primary radiation, *i.e.*

$$S_{p,bld}(E) = \frac{\dot{K}_{p,bld}(E)}{\dot{K}_{p,ref}(E)}, \tag{8}$$

[9] The method of *in situ* high resolution gamma spectrometry has been described by several authors (*e.g.* Boson, 2008)

where index *(p)* denotes that the quantity under consideration is due to primary photons of energy (E) from an artificial source (*e.g.* from fallout particles). For monoenergetic photons of energy *(E)* the primary kerma rate can be written as

$$\dot{K}_p = E\left(\frac{\mu_{tr}}{\rho}\right)_E \phi_p. \tag{9}$$

Since the kerma rate $\dot{K}_p$ is proportional to the primary fluence rate the shielding factor for primary radiation can be expressed as

$$S_{p,bld}(E) = \frac{\phi_{p,bld}(E)}{\phi_{p,ref}(E)}, \tag{10}$$

where $\phi_{p,bld}(E)$ is the primary photon fluence rate at a specific point in the building and $\phi_{p,ref}(E)$ is the primary photon fluence rate one meter above an infinite, plane source. Provided that the detector used to register the photons has a uniform efficiency in the lower half sphere and that the ground roughness may be approximated by being equal to unity, the shielding factor for primary radiation may be written as

$$S_{p,bld}(E) \approx \frac{\dot{N}_{bld}(E)}{\dot{N}_{gnd}(E)}, \tag{11}$$

where $\dot{N}_{bld}(E)$ is the registered count rate in the full energy peak inside a building due to an artificial source of gamma radiation outside the house and $\dot{N}_{gnd}(E)$ is the corresponding response to the same gamma source without the presence of the building. To incorporate the effect of scattered radiation from building materials and to obtain an assessment of the shielding factor (S_{bld}), the shielding factor for primary fluence is multiplied by a buildup factor, *i.e.*

$$S_{bld} = S_{p,bld}(E) \cdot B_{bld}, \tag{12}$$

where (B_{bld}) is a buildup factor larger than one (Finck, 1992).

2.3.2 Estimating the buildup factor

Several approximations are used to estimate the buildup factor in Eq. (12). Ultimately, the obtained buildup factor will depend on the area of the room in which the measurements were carried out. It will also depend on the detector height above ground when mounted in the building and the value of the measured shielding factor for the primary fluence.

The shielding factor for primary fluence may be considered as a combination of two shielding factors, the shielding factor for the geometric effect $(S_{p,geom})$ and the shielding factor for the building material effect $(S_{p,mtrl})$. This is expressed by Finck (1992) as

$$S_{p,bld} = S_{p,geom} \cdot S_{p,mtrl}. \tag{13}$$

The absence of fallout particles on the floor inside the building and the elevation of the detector when placed indoors will give rise to a different radiation field at the detector (compared to the standard height of one meter above ground when measuring without the building). This effect is purely geometrical and is incorporated in $(S_{p,geom})$. The shielding factor for the geometric effect is defined as:

$$S_{p,geom} = \frac{\phi_{p,geom}}{\phi_{p,gnd}}, \tag{14}$$

where $\phi_{p,geom}(E)$ is the primary photon fluence rate at the corresponding source position inside a building (or room inside a building) with the same dimensions as the building being investigated but with zero mass thickness *(ρx)* and $\phi_{p,gnd}(E)$ is the primary photon fluence rate one meter above ground (illustrated in Fig. 2).

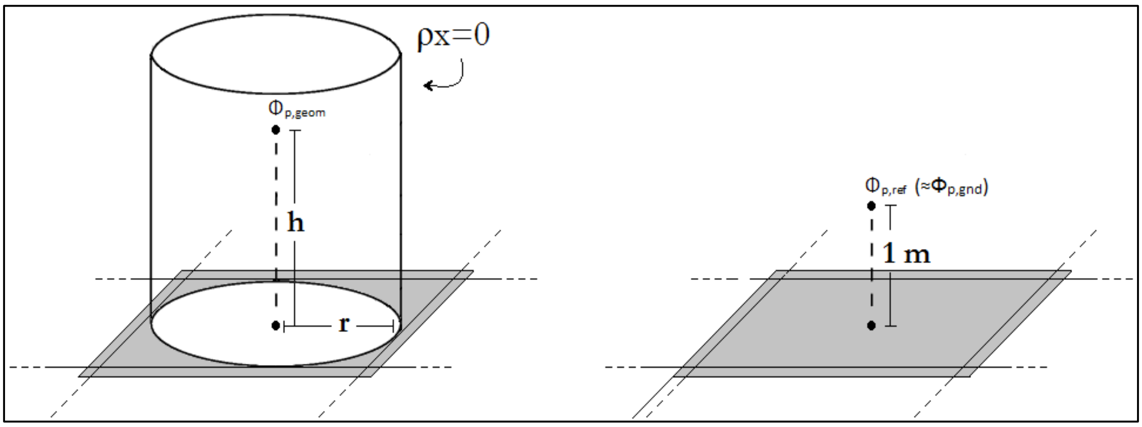

Figure 2: Illustration of the variables constituting the geometric shielding factor for a simple geometry. The grey quadratic area represents a contaminated surface and the circular area is used to approximately model the uncontaminated area covered by the building. Notice that the building has zero mass thickness.

As in the work of Finck (1992), a calculated value of the shielding factor for the geometric effect ($S_{p,geom}$) will be used to acquire the buildup factor for the specific building. Values of ($S_{p,geom}$) are given in Table 1 for the geometry depicted in Fig. 2, surrounded by a plane source of radioactive particles emitting photons of 662 keV.

Table 1: Geometric shielding factors ($S_{p,\ geom}$) calculated for an infinite plane ^{137}Cs source of 662 keV photons, as determined at different heights above the ground for different areas of the house (cleared radius). The table is reproduced from Finck (1992), with the kind permission of R. R. Finck.

Height (m)	**1**	**4**	**7**	**10**
Cleared radius (m)				
0	1.00	0.67	0.54	0.46
2	0.81	0.64	0.53	0.46
4	0.66	0.59	0.51	0.44
7	0.54	0.51	0.46	0.42
10	0.46	0.44	0.42	0.38

The material shielding factor can be expressed as

$$S_{p,mtrl} \equiv \frac{\phi_{p,bld}}{\phi_{p,geom}}. \tag{15}$$

where $\phi_{p,bld}(E)$ is the primary photon fluence rate at the source position inside the building (or room inside a building) and $\phi_{p,geom}(E)$ is the corresponding fluence rate for the building with zero mass-thickness (see Eq. (14)). The material shielding factor can be obtained from the measured shielding factor for primary radiation and the calculated geometrical shielding through the following approximation:

$$\frac{S_{p,bld}}{S_{p,geom}} = \frac{S_{gnd}\frac{\phi_{p,bld}}{\phi_{p,gnd}}}{\frac{\phi_{p,geom}}{\phi_{p,gnd}}} = S_{gnd}\frac{\phi_{p,bld}}{\phi_{p,geom}} \approx \frac{\phi_{p,bld}}{\phi_{p,geom}} = S_{p,mtrl}. \tag{16}$$

Now, the exponential attenuation law can be expressed as

$$\mu x = -ln\left(\frac{\phi}{\phi_0}\right), \tag{17}$$

where ϕ_0 is the fluence rate incident perpendicular on the shielding material (*e.g.* a wall) of average linear attenuation coefficient *(μ)* and *(ϕ)* is the transmitted fluence rate. Replacing the argument in Eq. (17) by the right hand side of Eq. (16) yields

$$\mu x = -ln\left(\frac{\phi}{\phi_0}\right) = -ln\left(\frac{\phi_{p,bld}}{\phi_{p,geom}}\right) = -ln\left(\frac{S_{p,bld}}{S_{p,geom}}\right). \tag{18}$$

Equation (18) yields the average building thickness in terms of mean free path units *(μx)*. The resulting mean free path of Eq. (18) can be used as input to calculate the buildup factor *(B_{bld})* needed in Eq. (12) to calculate the shielding factor *(S_{bld})*. Buildup factors as a function of mean free path have been published by Biro (1968). The published buildup factors have been calculated for monoenergetic photon fields between 0.2-10 MeV incidents on concrete. The use of these buildup factors relies on the fact that the most common building materials have a similar mass attenuation coefficient (DCPA, 1976).

Thus, by determining the primary shielding factor, the area of the building (or room inside the building) and the detector height above ground, the *in situ* method makes it possible to calculate the shielding factor.

3 Point source and limited source area approximations

According to the definition of the shielding factor, the kerma rate determined inside of a building is to be divided by the kerma rate registered one meter above the ground in the same source geometry (Eisenhauer, 1964). A first approximation that must be performed in an actual *in situ* measurement of the shielding factor is to replace the requirement of measuring the kerma rate above an infinite plane source by measuring it above a finite surface proximate to the building. This approximation presupposes that the radiation field above the proximal surface corresponds to the radiation field that would be present one meter above the ground at the same location as the building but in the absence of any building material. This approximation is valid if the deposition of radionuclides is homogeneously distributed over the fallout region and if the terrain is not too uneven (*i.e.* the shielding factor *(S_{gnd})* can be set equal to one). By using high resolution gamma spectrometry, and subtracting the natural background from the artificial background, the requirement of measuring the kerma rate (or fluence rate) at a nearby surface may be substituted by laboratory measurements on multiple point sources in an environment with minimal scattering from surrounding equipment.

However, it should be noted that real fallout is rarely deposited homogeneously and that large fluctuations (a factor of 5-10, or even more) in the deposited activity can be seen over both large regions (city or village) as well in smaller areas (gardens) (Bernhardsson, 2011).

3.1 Finite versus infinite plane source – fluence rate

Since the ratio of two different fluence rates, with and without a building present (K_{bld} and K_{gnd} respectively), are included in both the shielding factor (S_{bld}) as well as the shielding factor for primary radiation ($S_{p,bld}$), the error introduced by using a finite area when measuring the fluence rate will partly be balanced out.

Since the primary kerma rate is proportional to the primary fluence rate (see Eq. (9)), the fluence rate may be used to assess the discrepancy between using a finite source instead of an infinite. The resulting fluence rate at a point (P), located at a height (h) above an infinite plane source (Fig. 3) has been derived analytically by several authors (*e.g.* Kovalev and Foderaro., 1968; Kock, 2012).

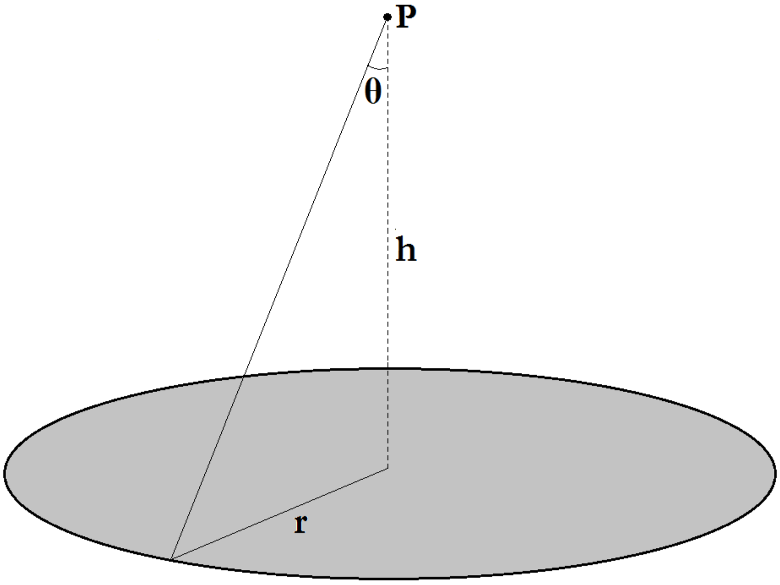

Figure 3: Geometry used when calculating primary fluence rate according to Eq. (17), with the detector in point (P) at height (h) above the ground.

The primary fluence rate above an infinite plane source can be written as

$$\dot{\phi} = \frac{S_A}{2} \int_{\mu_a \cdot h}^{\infty} \frac{exp(-t)}{t} dt, \qquad (19)$$

where (μ_a) is the linear attenuation coefficient in air for a given energy, (S_A) is the source strength (activity per unit area) and $t = (\mu_a \cdot h)/cos(\theta)$ (Kock, 2012). The integral in Eq. (19) is an exponential integral (denoted $E_1(\mu_a \cdot h)$) and cannot evaluated using elementary functions (Geller and Edward, 1969). To evaluate the difference in primary fluence rate at point (P) due to a finite plane source of radius (r) and an infinite plane source (where both surfaces has equal source strength (S_A)) numerical methods must be applied. Using the linear attenuation coefficient in air for photons of energy 662 keV (^{137}Cs, μ_a= 9.34·10^{-5} cm^{-1}), it is seen that when the radius of the plane source is 600 m approximately the same fluence rate arises at point (P) (a relative difference of less than 1.5·10^{-5} is obtained for r=600 m). In practice, a radius of 600 m is far too large to be used when conducting a fallout simulation with the aid of point sources. However, almost 90% of the primary photons that reach P are from sources within a radius of 60 m (Isaksson, 2011).

3.2 Point source versus extended source – source strength

The method of approximating a plane source with multiple point sources is necessary in order to obtain permission to experimentally simulate fallout of long lived radioisotopes such as ^{137}Cs ($t_{1/2}$ = 30.17 y), since the Swedish Radiation Safety Authority (SSM) have stipulated that no more than 10 kBq of ^{137}Cs may be released into the environment, at a maximum of four occasions per month (SSM, 2010). Since the activity needed to get a sufficient detector response is in the order of hundreds of MBq, sealed sources (that will not disperse any activity to the environment) must be used in order to experimentally determine shielding factors.

Given a point detector, the error introduced when replacing a plane disc source with a point source is less than 10% when calculating the fluence rate, provided that the distance between the detector and the source is approximately 2.2 times the radius of the disc source (Isaksson, 2011). Similar calculations have been made by other authors. Bevelacqua (2005) estimated that a percentage difference of less than 1% could be achieved when using a points source instead of disc sources if the distance between the source and the point detector were at least 3 times the distance of the diameter of the disc source. Generally, the smaller the solid angle of the source relative to the detector, the better the approximation becomes of replacing an extended source with a point source. By utilizing the fact that a detector cannot "see" the difference between a point source and an extended source, given a certain distance, a schematic arrangement of point sources may be used to simulate fallout on a surface, as illustrated in Fig 4.

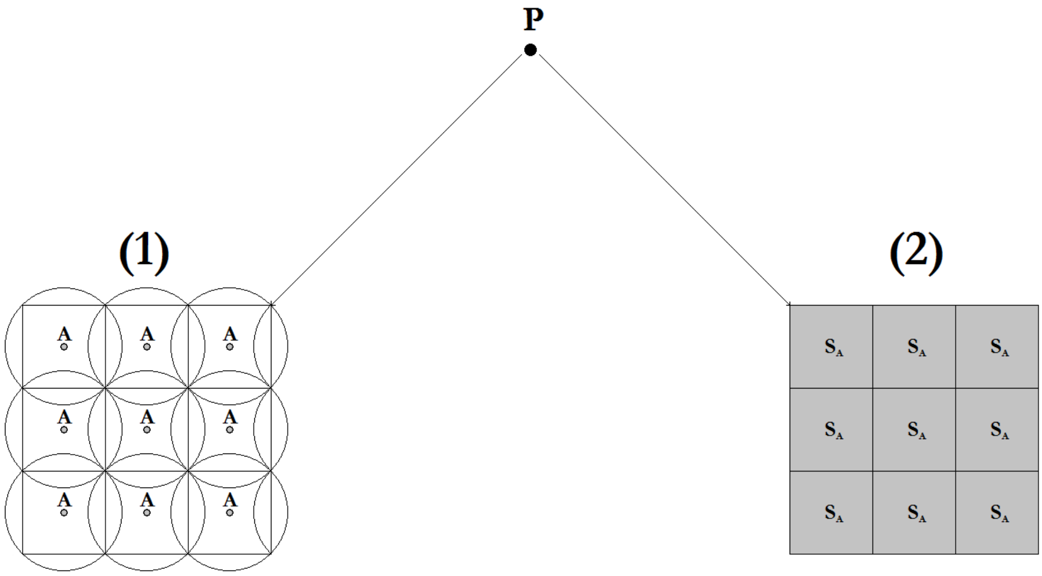

Figure 4: Schematic illustration of the point source approximation. A point source of activity *(A)* is placed at the center of each disc in (1). Each disc encloses a square of area l^2 and the radius of the discs becomes $(l/\sqrt{2})$. In (2) the activity of each square has been distributed over its respective area giving rise to a source activity of $S_A = A/l^2$ per square. Given that the distance between P and (1) and (2), respectively, is at least $3\times\sqrt{2}l$, the error will approximately be less than 1% when (2) is replaced with (1).

3.3 Symmetry – reduction of source positions

To reduce the number of source positions needed when simulating a fallout, the approximation that many buildings can be considered as symmetric over certain axes is utilized (Fig. 5).

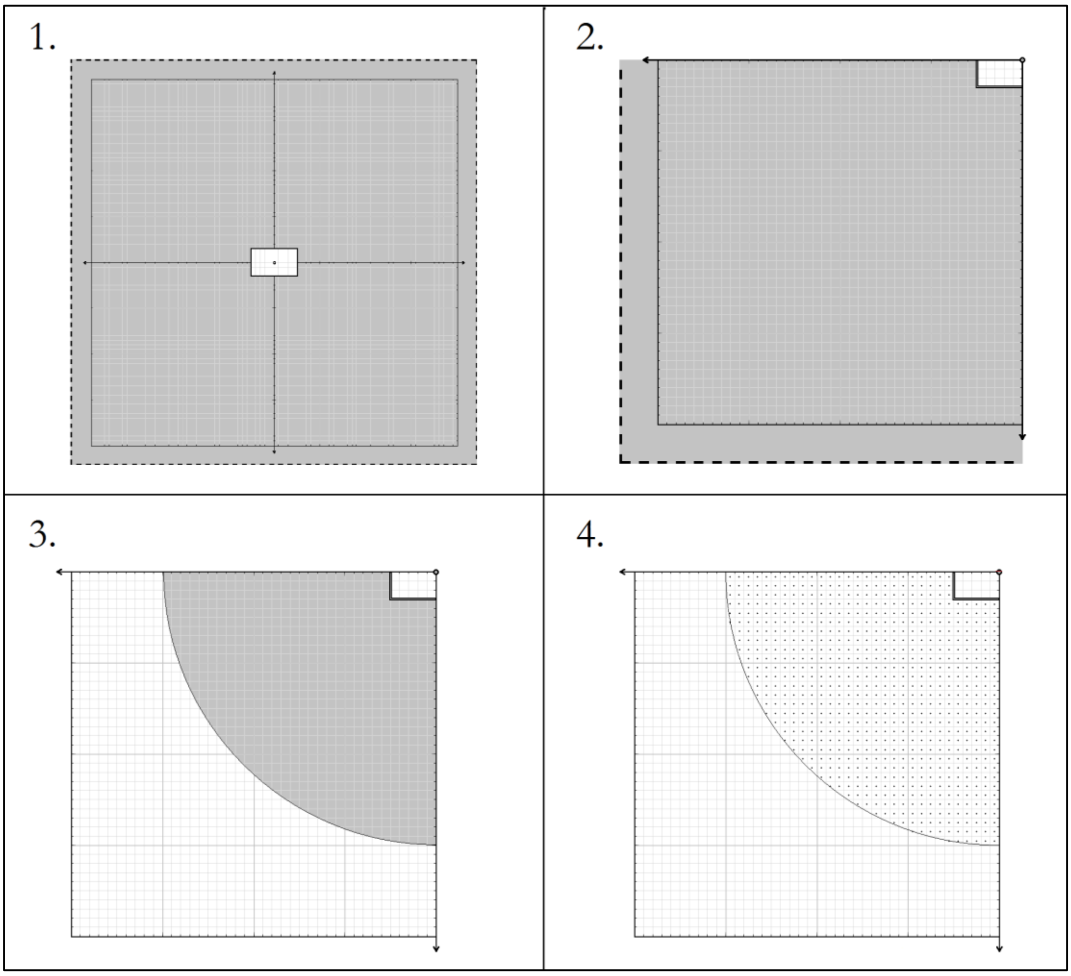

Figure 5: Schematic illustration of the sequence of successive approximations underlying the fallout simulation. 1: box-shaped building surrounded by infinite plane source of homogeneously deposited radionuclides. 2: symmetry considerations reduces the infinite plane source to a semi-infinite plane source using a quarter of the building. 3: circle sector of finite radius and with the same source strength as in (1) and (2). 4: point sources positioned symmetrically to give rise to the same activity per unit area (*i.e.* source strength) as in (3).

With reference to Fig. 5, the following steps summarize the approximations carried out to reduce the number of point sources needed:

1. The building may be viewed as a box-shaped structure with a rectangular base. This building is in turn surrounded by an infinite, homogeneous plane source of ^{137}Cs.

2. Provided that the internal structures in the building are symmetrically distributed (or that the house consists only of walls and roof), the kerma rate at a height of 1 m above the floor in the center of the building (frame 1., in Fig. 5) is equal to four times the kerma rate from one quadrant (frame 2., in Fig. 5), *i.e.*, only a semi-infinite plane has to be considered (one fourth of a plane).

3. In the absence of a building, the flux of photons from radiation sources positioned on the same radial distance with respect to the center of the circle will be equally reduced (due to attenuation in air and the inverse-square relation). As discussed earlier (see Ch. 3.1) 90% of the contribution to the fluence rate comes from sources within a 60 meter radius. Thus, given a sufficiently large radius the contribution from the outermost sources will be approximately negligible. Hence, the semi-infinite quadrant of ground deposited fallout can be approximated with a finite circle sector of sufficiently large radius and with the same deposition density as the infinite plane source.

4. Now, according to Ch. 3.2, provided that the distance from the center of the building to the outer walls is sufficiently large, a detector positioned at the center of the building will not be able to detect the difference between the flux of photons from a quadratic photon source of area ($\Delta x_i \times \Delta x_j$) and a photon point source positioned at the center of a square (where the activity divided by the area of the square is numerically equal to the source strength of the quadratic source). Thus, the extended source may be replaced with multiple point sources positioned symmetrically inside the finite circle sector.

Furthermore, if a long lived (half-life sufficiently long compared to the duration of the experiment) radionuclide such as ^{137}Cs is used and if the detector have a stable response over time (or this can be compensated for), a single point source can be positioned at one point (frame 4., in Fig. 5) at a time, and a spectrum acquired for each point under equal time duration. This can be achieved so that all points within the circle sector are covered. By calculating the resulting count rate from all points, and by measuring the corresponding points without a house present, the quantities necessary to calculate the primary shielding factor $(S_{p,bld})$ will be obtained.

4 Materials and Methods

4.1 Test site – location and house type

A field test of the *in situ* spectrometric method of measuring shielding factors was made possible by borrowing a building, and associated land, from the Swedish Armed Forces, division P7 at Revingehed. A farm house located on P7s exercise and artillery range was made available (Fig. 6).

Figure 6: Photos from different views of the Fredrikslund estate at Revingehed (referred to as "trial building"). Upper left: Aerial view of the trial house. Area encompassed by the red circle sector indicates the area where fallout simulation was performed. Upper right: Trial house as viewed from the center of the fallout-simulation area. Lower left: Side view of the trial building. This picture shows the short-side of the room for which the shielding factors were measured. Lower right: Side view of trial building. This picture shows the long-side of the room for which the shielding factors were measured.

The trial building is an old farm house that was renovated during the 1930s. The building has concrete floor and is constructed with thick walls (approximately 0.4 m thick) of bricks and the wall mass thickness is approximately 540 kg/m^2. The classification of the house according to the Swedish Civil Defence Administration has not been identified. However, given the design of the house it is assumed that it will have shielding coefficients similar to the building categorized as a F3 building[10] (Danielsson *et al.*, 1984)

4.2 Fallout simulation – point source arrangement

Figure 7 shows that a ^{137}Cs-source located at radial distance of 30 m from the center of the building contributes with a photon flux approximately equal to 1% of the primary flux of 662 keV photons as compared to a point source positioned close to the outside wall of the building, given that attenuation in the building material is not considered. Furthermore, the relative difference in fluence rate between a disc source of radius 30 m and an infinite plane source (Eq. (17)), of the same source strength, will be less than 25%.

[10] F3: House usually built in the 1940s with thick brick walls and concrete floor.

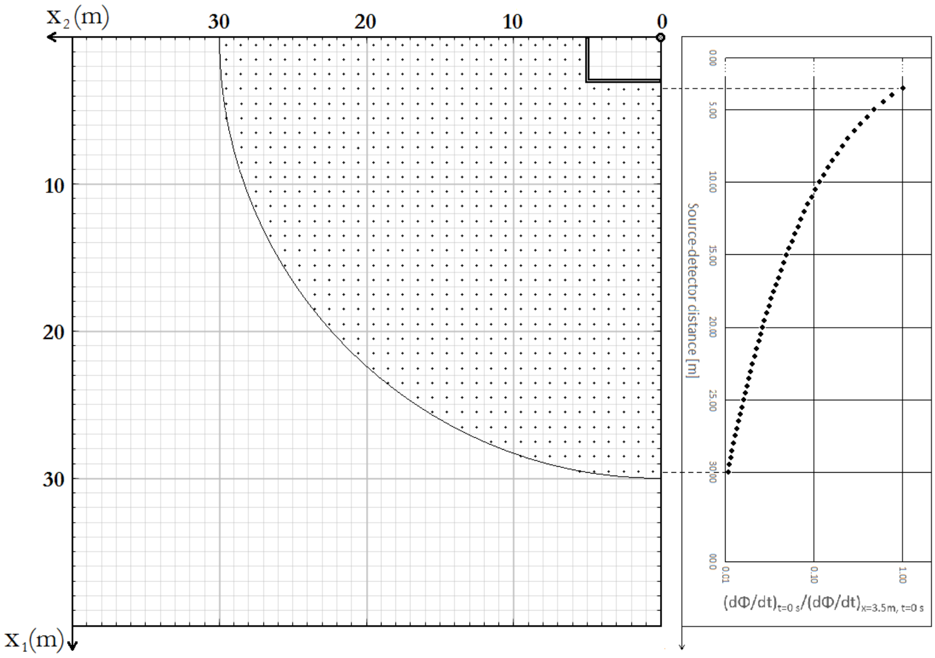

Figure 7: Left: Schematic illustration of the positions for the point source (dots) during the measurement of the shielding factor. The X_2-direction is designated as "columns" and the X_1-directions are designated as "rows". The flux of 662 keV photons at the center of the building from a point source positioned at a distance (x_1, x_2) from the center, normalized to the contribution from the point source when positioned at the nearest position to the detector (right).

The approximations discussed in Ch. 3 were used when calculating the number of positions for the ^{137}Cs-source outside of the trial building. A circle sector of a 30 m radius was calculated to encompass approximately 700 points. Inside the circle sector each sampling point represent an area of (1 m × 1 m), at a specific distance from the source position inside the trial building (Fig. 7). Due to moving the source and data storage between each source movement, the approximated time for the experiment described is: 700 positions × 1.5 min = 1050 min = 17.5 h. If the same person is moving the source, this person will be exposed (closer than 1 m) to the source less than 1 h. As an example, for a 150 MBq ^{137}Cs source the effective dose due to this experiment is expected to be approximately 15 μSv.

4.3 Measurements

The field measurements were carried out between the 16th and 19th of December 2013. A high-purity germanium (HPGe) detector from Ortec[11], with a relative efficiency[12] of 123% was used. A DigiDART (EG&G Ortec) was used as a spectrum analyzer, coupled to a PC for data storage. The detector system was mounted on a tripod and positioned centrally in one of the corner rooms in the trial building (Fig. 8). A number of different radiation protection instruments (GR100 and GR110 from SAIC Exploranium[13]; SRV200 from RADOS[14]) were also used inside the building to monitor the dose rate variation at the different positions of the source outside the house.

[11] Ortec, 801 S. Illinois Ave., Oak Ridge, TN, USA.
[12] At 1.33 MeV (^{60}Co).
[13] SAIC Exploranium, 6108 Edwards Blvd, Mississauga, ON, Canada.
[14] Mirion Technologies (RADOS), Mustionkatu 2, 20750 Turku, Finland

Figure 8: HPGe detector positioned in the center of the corner room of the house, and images showing the HPGe detector facing the corner towards the fallout area (left frame); the HPGe detector facing the short side of the room with a window (right frame). Note that the cryostat is mounted above detector to minimize shielding of ground emitted photons.

The fallout simulation was carried out by positioning a ^{137}Cs-source[15] of 156 MBq on the designated source positions; starting with the top row, increasing the column value X_2 until one row was fully covered and then starting over the process on the next row until all the source positions were covered. For the first three lines, and for all source positions within a 5 meter radius of the house, measurements were performed. However, starting from row four every other source position was omitted in order the cover the whole measuring area (Fig. 9) during the disposal period of the trial building. The Cs-source was mounted on a metal rod that was put down in the soil, to assure the same height above ground at each position. This height was also used to minimize the influence of ground roughness over the surface.

[15] Enclosed in a thin, water-proof metal container.

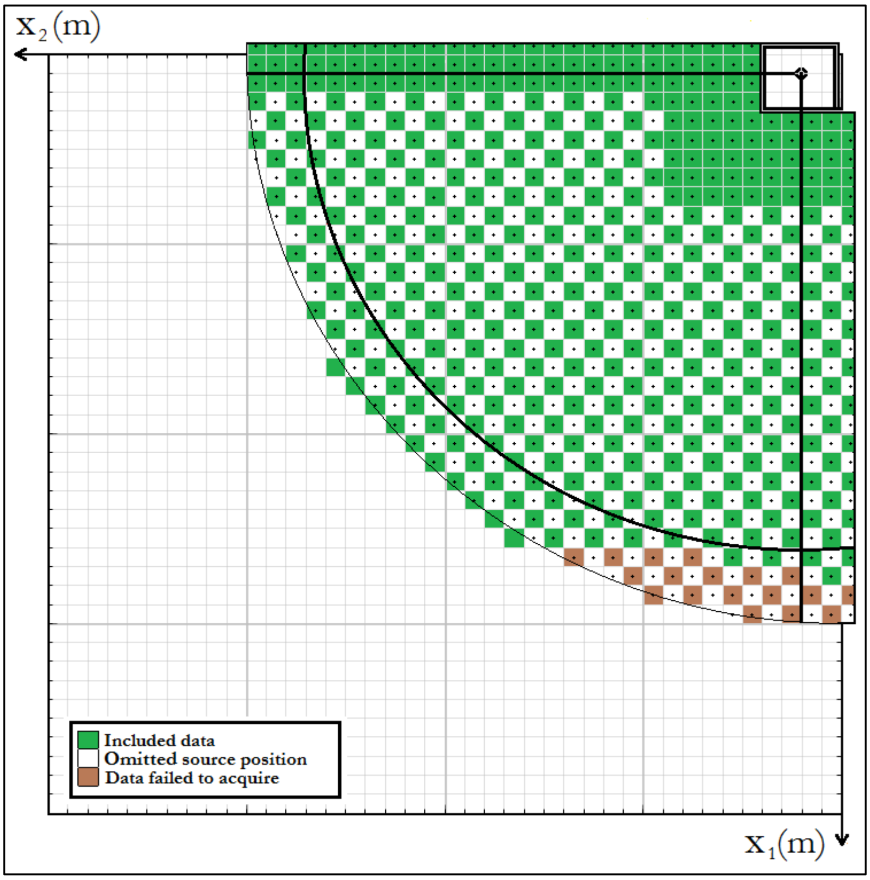

Figure 9: Source positions that were covered during the field trial of the *in situ* spectrometric method for determining shielding factors. Description of the different colors is given in the figure label.

Each position of the Cs-source had been carefully marked out (Fig. 10) before any measurements were conducted on the surface. The estimated accuracy of this positioning system was determined to ±0.1 m.

Figure 10: Markers for the position of the Cs-source (orange sticks).

The gamma radiation background was acquired inside the trial building for 1.25 h. The obtained value was used as background correction for all source positions. A measurement time of 2 min (detector live time) was used for all source positions. The obtained full energy peak areas were corrected for background radiation and summed, yielding a count rate ($\dot{N}_{bld}$) in the full energy peak with a statistical uncertainty of 0.2%. The outdoor count rate ($\dot{N}_{gnd}$) was determined in the laboratory by measuring the count rate from corresponding distances as the source positions in the field trial.

The values obtained were not corrected for the angular efficiency of the detector. However, the detector used in the present study is known to have an angular efficiency, at 662 keV that varies less than 6% from 0° to 90° degrees (photons incident perpendicular to the short side of the detector casing and to the long side of the detector casing, respectively).

The shielding factor for primary fluence was obtained through Eq. (11). By measuring the area of the floor inside the trial building, a geometrical shielding factor could be calculated by means of interpolation (Table 1). Using the average building thickness, obtained from Eq. (18) a buildup factor could be obtained from the tables published by Biro (1968). The shielding factor of the building, according to the *in situ* spectrometric method, was thereafter calculated according to Eq. (12).

5 Results and Discussion

5.1 Primary and scattered photons as registered inside the house at different source distances

The number of photons registered in the full energy peak of ^{137}Cs (662 keV) varies with distance between the source and the detector. This difference was determined by measurements at Fredrikslund and from laboratory measurements, respectively. The resulting number of counts in the full energy peak (corrected for background), collected during a measurement time 120 s (detector live time), were plotted for corresponding distances from the detector (Fig. 11) in order to assess how the different source positions contributed to the primary fluence rate.

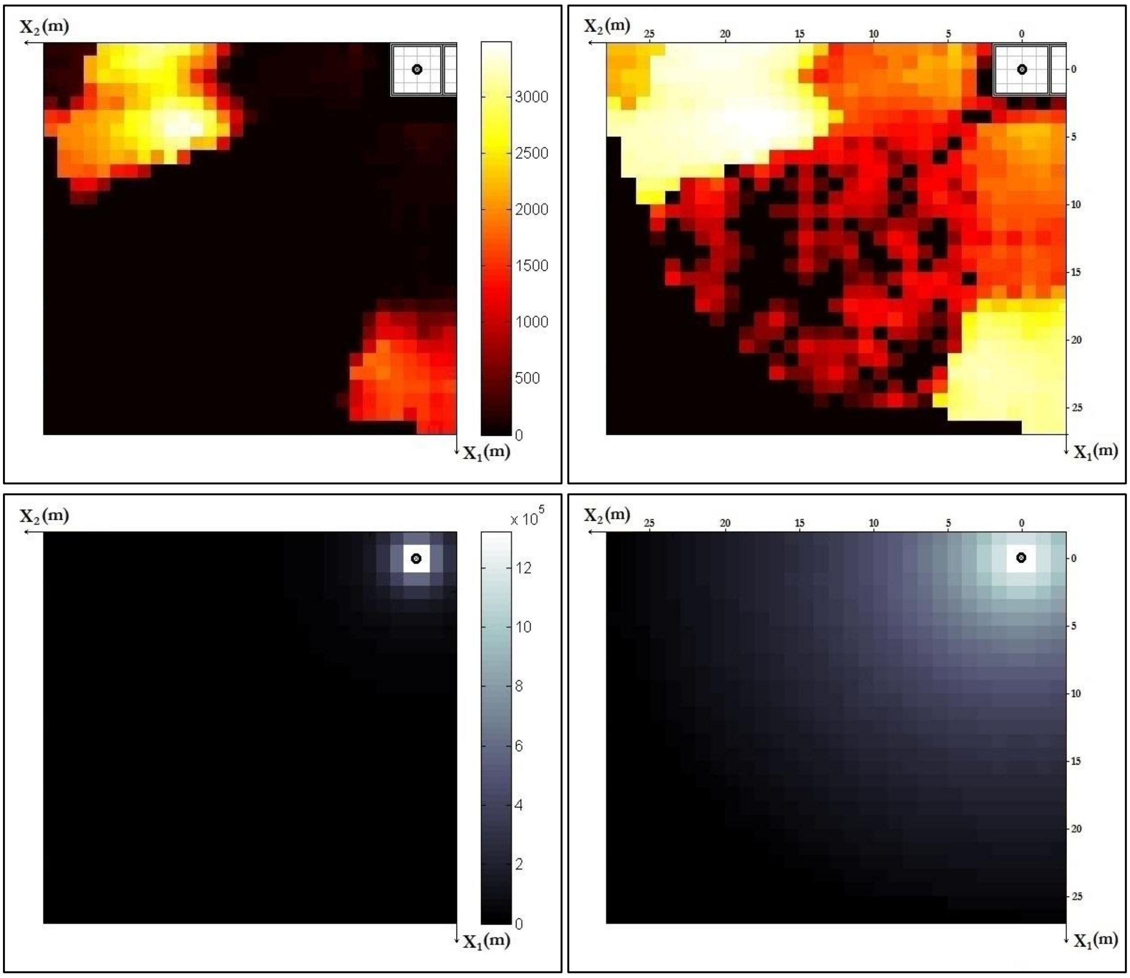

Figure 11: The net count in the full energy peak of ^{137}Cs due to a point source of 156 MBq positioned at different distances from the detector (located inside the house, indicated by a black circle). Omitted source positions (see Fig. 9) inside the circle sector were taken as the arithmetic mean of adjacent data points. Upper left frame: net counts registered 1 m above the floor inside the corner room of the trial building. Upper right frame: the logarithm of the number of net counts registered in the trial building. Lower left frame: net counts registered 1 m above ground without the presence of a building. Lower right frame: the logarithm of the number of net counts registered 1 m above ground without the presence of a building.

Looking at the upper diagrams of Fig. 11, the number of primary photons detected does not seem to decrease with the square of the distance to the detector. Furthermore, the main contribution to the primary fluence at the detector appears to come from source positions at approximately 20 m distance from the short and long side of the house, respectively. This behavior is not observed in the lower diagrams of Fig. 11. This may be explained by two factors, the windows on the long- and short sides of the house and the height of the windows above the ground (Fig. 12). Photons emitted from a distance of approx. 20 m travel in a straight line from the source to the detector through air and a thin window. At source distances closer to the house the photons are more attenuated as they have to pass the relatively thick walls of bricks before they are registered in the detector. Additionally, it should be noted that the number of counts can be up to five orders of magnitude larger in the absence of the house for source positions at equal distances from the detector (Fig 11; lower left).

Now, to explain why the main contribution of primary 662 keV photons emerges at a certain distance from the house (*i.e.* "does not follow" the inverse-square relation) consider Fig. 12.

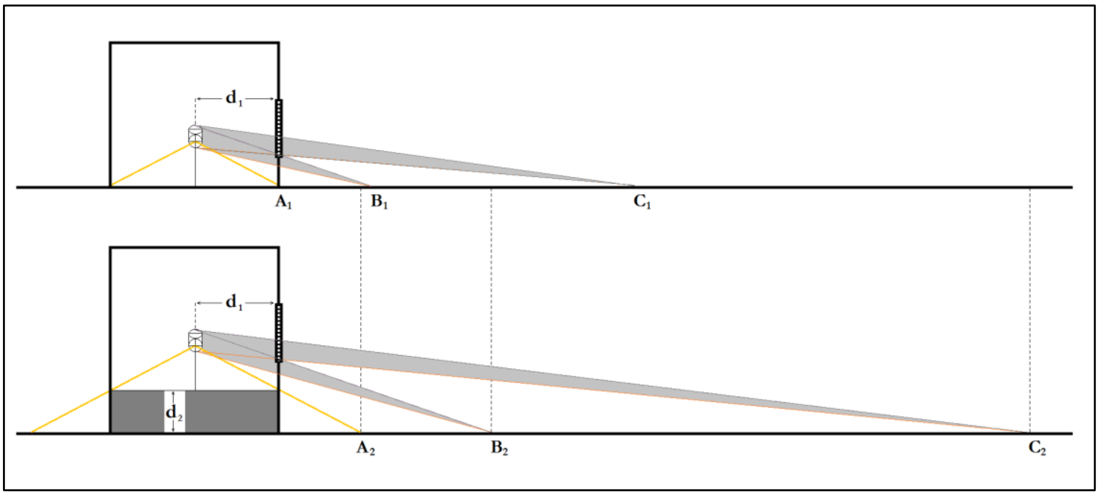

Figure 12: Cross-section of the house at the position of the window, standing at different heights above the horizontal ground (upper frame: $d_2 = 0$ m; lower frame: $d_2 = 0.7$ m). The influence of floor height above ground, wall-shielding and detector size on the number of primary photons detected inside the house from a point source outside (the detector size is exaggerated for purposes of illustration). Upper frame: detector of finite length positioned at some distance *(d_1)* from the window and with floor at the same height as the ^{137}Cs-contaminated ground outside the building. Lower frame: same configurations as in the upper diagram, apart from an elevation *(d_2)* of the floor relative to the ground. Source positions are denoted A_1, A_2 and B_1, B_2, respectively.

Since there is no contamination of ^{137}Cs on the floor inside the house (Fig. 12), the source closest to the house that will have photons reaching the detector will be located at A_1 and A_2, respectively. As the windows are located at a certain height above the ground, photons emerging from sources between A_1 - B_1 and A_2 - B_2 must travel through the wall to reach the detector. On the other hand, photons emerging from (B_1 or B_2) will hit the detector by passing through the window. Hence, given that the mass thickness of the wall is sufficiently large and that photons are emitted isotropicly from the ^{137}Cs-source, an increase in count rate is expected at (B_1 and B_2). Further, the solid angle subtended by the detector at a point source located between, *e.g.*, (B_1) and (C_1) will become larger as the source approaches (C_1). If attenuation in air and the inverse-square relation is ignored, a maximum count rate of primary photons would be registered at (C_1)[16], followed by approximately a constant number of counts for source locations further away. Elevating the floor a height (d_2) will displace (A_1) into (A_2), (B_1) into (B_2) and (C_1) into (C_2). As a consequence the theoretical "maximum" will be displaced further away from the building. The distance to the theoretical maximum was not calculated prior to the conducted measurements since access to the building was limited. Nevertheless, using the measurements of the house dimensions (thickness of walls, floor elevation) and a detector length of 0.08 m as parameters, a graphical method yielded a theoretical maximum, positioned 23 m from the building wall.

In contrast to the appearance of the upper diagrams of Fig. 11, the total number of counts in the Compton continuum of 662 keV photons (0-477 keV, for ^{137}Cs) appears to have a quadratic dependence on detector distance (Fig. 13).

[16] Ignoring the angular efficiency of the detector.

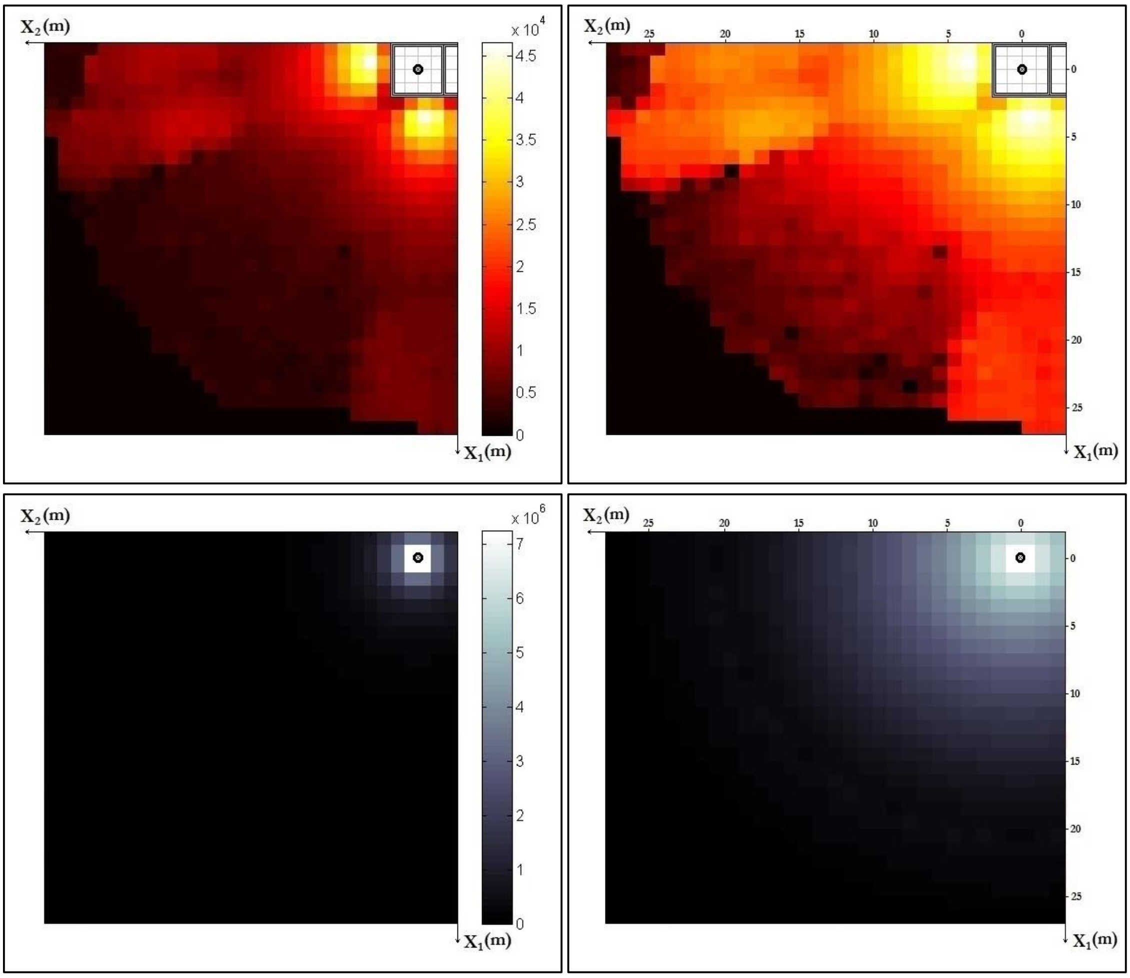

Figure 13: The net counts in the Compton continuum of 662 keV photons due to a point source of 156 MBq positioned at different distances from the detector (indicated by a black circle). Omitted source positions (see Fig. 9) on the surface were taken as the arithmetic mean of adjacent data points. Upper left frame: net counts registered 1 m above the floor inside the corner room of the trial building. Upper right frame: the logarithm of the number of net counts registered in the trial building. Lower left frame: net counts registered 1 m above ground without the presence of a building. Lower right frame: the logarithm of the number of net counts registered 1 m above ground without the presence of a building.

The difference in number of counts, when comparing the Compton part of the spectrum with and without a building present, can be up to approximately two orders of magnitude for source positions at equal distances.

The knowledge on the contribution from different source positions to the primary fluence rate at the detector can be useful when calculating the shielding factors. This is important to know since it makes it possible to analyze how the geometry of the surroundings and the house itself affects the radiation fields. This is especially useful in order to reduce uncertainties associated with, *e.g.*, deposition density. For example, when measuring shielding factors according to the *in situ* spectrometric method on a real fallout, variations in deposition density, depth distribution, combined with a limited number of fluence-rate measurements, give rise to high uncertainties (Finck, 1992). By using point sources according to the described procedure, uncertainties due to differences in distribution density, depth distribution and ground roughness may be reduced to some degree.

The uncertainties introduced when using point sources must be assessed in order to evaluate the usefulness of the described procedure. These uncertainties have not been analyzed in the current work but must certainly be identified if shielding factors determined according to the point source method are to be used in any practical implementations (*e.g.,* as decision support following a nuclear power plant accident).

5.2 The shielding factor for primary fluence calculated for different source configurations

The total count rates in the full energy peak of ^{137}Cs ($\dot{N}_{bld}$ and $\dot{N}_{gnd}$, respectively) were calculated for three different source configurations (Fig. 14). This was done in order to investigate how different numbers of source positions affect the value of the shielding factor.

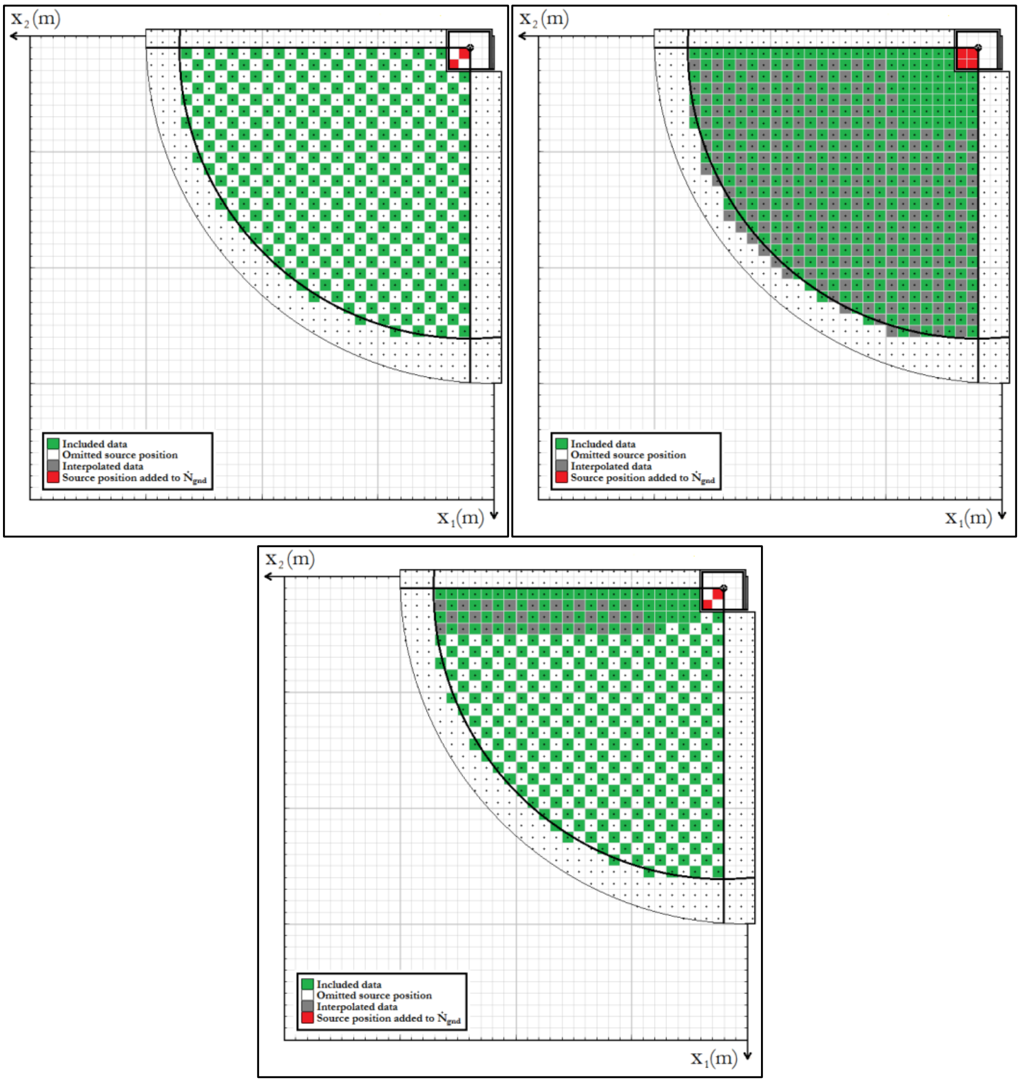

Figure 14: Source configurations used to calculate the total count rates $\dot{N}_{bld}(E)$ and $\dot{N}_{gnd}(E)$. Upper left frame: configuration denoted "100%." 256 source positions with a building present and 258 without the building, with an average source strength of 78 MBq·m^{-2}. Upper right frame: configuration denoted "200%." 512 source positions with a building present and 516 without the building, with an average source strength of 156 MBq·m^{-2}. Lower frame: configuration denoted "Inhomogeneous." 300 source positions with a building present and 302 without the building. Average source strength was not calculated for this case/situation. A description of the different colors used in the images is given in the figure labels.

Only random uncertainties were considered while calculating the count rate in the full energy peak for each source configuration. The random uncertainties in the total count rate were derived by error-propagation from the number of registered counts in the full energy peak. The resulting count rates are presented in Table 2 together with the corresponding value of the shielding factors for primary radiation (calculated according to Eq. (11)).

Table 2: Total count rate in the full energy peak due to different source configurations and the shielding factor for primary 662 keV photons. Uncertainties are given as one standard deviation. The values presented under the "Number of source positions" column refer to the source positions outside the building.

Source configuration	Number of source positions	$\dot{N}_{bld}$ (s^{-1})	$\dot{N}_{gnd}$ (s^{-1})	$S_{p,bld}$
100 %	256	997 ± 5	46880 ± 20	0.0213 ± 0.0001
200%	512	1960 ± 9	87850 ± 30	0.0223 ± 0.0001
Inhomogeneous	300	1426 ± 6	56921 ± 22	0.0250 ± 0.0001

Table 2 shows that the shielding factor for primary radiation $(S_{p,bld})$ is larger (*i.e.* the house offers less protection against primary radiation) for the "Inhomogeneous" source configuration than for the two other configurations. The reason why it becomes larger for this case is most likely due to the uneven distribution of activity, with higher source strength in a direction perpendicular to one of the windows. It has already been observed (Fig. 11, upper left frame) that the main contribution of primary radiation from ^{137}Cs comes from sources perpendicular to the windows. Thus, $(S_{p,bld})$ will become higher because of the unevenly distributed activity. The result from the "Inhomogeneous" case clearly demonstrates the need to position the source in a symmetrical manner in order to avoid uneven weighting of the primary fluence to the detector.

Furthermore, Table 2 shows that the difference in $(S_{p,bld})$ is less than 5% between the "100%" source configuration and the "200%" cases. One of the reasons that $(S_{p,bld})$ becomes smaller in the "100%" configuration is because source positions corresponding to the building floor will contribute more to $(\dot{N}_{gnd})$ in this case than in the "200%" configuration. Observing the raw data used to calculate the total count rate it can be seen that approximately 31% of the registered counts in the full energy peak is due to sources that are within the area corresponding to the building floor in the "100%" case and 28% in the "200%" case. Clearly, the inclusion/exclusion of source positions corresponding to the building floor is a crucial part when the shielding factor is calculated according to the *in situ* spectrometric method (combined with point sources) (see Eq. (12)) since these data points will form a substantial part of the calculated value.

Initially, $(S_{p,bld})$ was supposed to be investigated for source configurations of lower source strength (*i.e.* fewer source positions on the trial area). However, the floor area in the investigated part of the trial building (and the point/surface source approximation) limits the number of source points that can be omitted without distorting the calculated value of $(S_{p,bld})$. This problem was not further investigated in the present paper. Still, since it is desirable to reduce the number of source positions, and hence reducing the time needed to simulate a fallout, it will be of primary interest to further study this aspect of the point source method.

5.3 The shielding factor for the trial building

Two different values of the geometric shielding factor *($S_{p,geom}$)* were acquired by interpolation in Table 1. In both cases a detector height of 1.7 m was used as input value for “Height”. As input value for “Cleared radius” an estimate of the radius of the room was used for the first case and for the building in the second case. This was done in order to see the effect of the cleared area on the calculated shielding factor.

Table 3: Origin of radius, input radii for interpolation in Table 1 and resulting geometric shielding factor.

Area	Radius (m)	$S_{p,geom}$
Room floor	2.0	0.77
Building floor	15.5	0.51

Values of the average building thickness, in terms of mean free path units *(μx),* were calculated by combining *($S_{p,bld}$)* obtained from the “100%” and “200%” source configuration, respectively, with the *($S_{p,geom}$)* values of Table 3. The calculations were performed according to the procedure described in Ch. 2.3.2.

Using the calculated values of the average building thickness as input values, the buildup factors could be obtained through interpolation in the tables published by Biro (1968). Finally, multiplying the buildup factor with its associated shielding factor for primary fluence (Eq. 12), shielding factors corresponding to the two source configurations (“100%” and “200%”, respectively) could be calculated for the two cases of *($S_{p,geom}$)*. Results from these interpolations and calculation are presented in Table 4.

Table 4: Shielding factors calculated according to Eq. 12; Dose buildup factors *(B)* for 662 keV photons normally incident on concrete obtained from interpolation with calculated values of the average building thickness *(μx)*. Values of *($S_{p,bld}$)* and *($S_{p,geom}$)* were taken from Table 2 and 3, respectively.

Source configuration	$S_{p,geom}$	$S_{p,bld}$	μz	B	S_{bld}
100%	0.77	0.0213	3.6	4.66	0.099
100%	0.51	0.0213	3.2	4.22	0.090
200%	0.77	0.0223	3.5	4.61	0.10
200%	0.51	0.0223	3.1	4.16	0.093

No attempt to propagate the errors through the calculations and interpolations were performed for the results in Table 4 (excluding $S_{p,bld}$). Furthermore, systematic errors were not analyzed in the course of this paper Thus, the acquired values of *(S_{bld})* may only be viewed as indications rather than established values.

Nevertheless, since the uncertainties pertaining to activity distribution and ground roughness probably will be less than in the work by Finck and since the calculations of the buildup factor were performed in a similar manner it is not implausible that the overall uncertainties related to *(S_{bld})* could be of the same order as estimated by Finck (1992). Still, it would be erroneous to cite any uncertainty values since this must be properly investigated.

Under the assumption that the shielding factors In Table 4 do not have too large uncertainties, several results can be ascertained from the calculated values of *(S_{bld})*. First of all, reducing the number of source positions to half the value (*i.e.* using the "100%" source configuration instead of the "200%" configuration) will yield a difference in shielding factor that is less than 10%. This is a desirable result since it indicates that less source positions may be used to determine the shielding factor for a given building, which may potentially reduce the experimental time up to 50%. Furthermore, using the floor area instead of the house area yields a shielding factor that is approximately 10% larger for both cases of source configurations. Thus, if a conservative estimate of the shielding factor is required it may be better to consider the floor area instead of the building area when calculating the shielding factor according to the *in situ* spectrometric method (if no corrections for room placement in the building is performed).

6 Conclusions

A method of determining shielding factors through a combination of the *in situ* spectrometric method and point sources may be possible. The method can be performed without exceeding guideline values for dose. Calculations of the shielding factor for two different source configurations (number of source positions) indicates that it may be possible to reduce the time it takes to perform the method. However, further investigations are needed in order to establish the precision of the method and the uncertainties that the method imposes on the shielding factor.

7 Future aspects

Methods to experimentally assess the shielding factor for a given building must be developed. A method based on gamma spectrometry and point sources might be possible to conceive. In order to develop this method several aspects of the Standard Method must be adjusted to the existing technology and knowledge that gamma spectrometry has to offer. The work of adjusting and modernizing the concept of shielding factors is a long term project that will be able to contribute to improved knowledge and methodology in both measurement methods as well as population protection in terms of decontamination and relocation strategies after a radioactive fallout event.

Acknowledgements

This project was financially supported by the Swedish Radiation Safety Authority (SSM). Thanks are also due to Robert R. Finck for helpful discussions.

References

Attix, F.H., 2004. *Introduction to Radiological Physics and Radiation Dosimetry*. 2nd ed. Weinheim: Wiley-VCH Verlag GmbH & Co., 21-22.

Auxier, J.A., Buchanan, J.O., Eisenhauer, C. and Menker, H.E., 1959. *Experimental Evaluation of the Radiation Protection Afforded by Residential Structures Against Distributed Sources.* CEX-58.1. Oak Ridge, TN, U.S. Atomic Energy Commission. Civil Effects Test Operations Office. 133 pages.

Bernhardsson, C., 2011. *Radiation exposure of human populations in villages in Russia and Belarus affected by fallout from the Chernobyl reactor – Measurements using optically stimulated luminescence in NaCl, TL-dosemeters and portable survey instruments.* Thesis (PhD). Department of Medical Radiation Physics, Malmö, Lund University, Sweden.

Bevelacqua, J.J., 2005. Point Source Approximations in Health Physics. RSO Magazine, 10 (1), 19-23.

Biro, G.G., 1968. Application of the Monte Carlo Method to Shielding *In:* Jaeger, R.G., ed. *Engineering Compendium on Radiation Shielding. Volume I – Shielding Fundamentals and Methods*. Berlin: Springer-Verlag, 105-106.

Boson, J., 2008. *Improving accuracy of in situ gamma-ray spectrometry.* Thesis (PhD). Department of Radiation Sciences, Radiation Physics, Umeå University, Sweden.

Burson, Z.G., 1969. *Experimental Evaluation of the Fallout-Radiation Protection Provided by Structures in the Control Point Area of the Nevada Test Site*. CEX-69.5. Washington, D.C., United States. Dept. of Energy. 120 pages.

Danielson, G., Dellgar, U., Lindqvist, S., Schyllander, J., 1984. *Svenska bostadshus. Befolkningsfördelning och skyddsfaktorer för radioaktivt nedfall (Swedish Dwellings. Population Distribution and Shielding Factors for Radioactive Fallout).* Cfs 1.04-94 FK. Karlstad, Swedish Civil Defence Administration, Karlstad.

DCPA, 1976. *Shelter Design and Analysis – Fallout Radiation Shielding*. TR-20, Vol. 1 (Rev. Ed.). Washington, D.C., Defense Civil Preparedness Agency. 360 pages.

Eisenhauer, 1964. *An Engineering Method for Calculating Protection Afforded by Structures Against Fallout Radiation*. National Bureau of Standards Monograph 76. Washington, D.C., U.S. Government Printing Office. 134 pages.

Elvers, E., Nilsson, M. and Danielson G., 1979. *KVAST – ett datorprogram för beräkning av byggnaders skyddsfaktorer för kvarvarande strålning (KVAST – A Computer Program for Calculation of Building Shielding Factors for Fallout Radiation).* FOA C20321-A2. Stockholm, Swedish Defense Research Establishment.

Finck, R.R., 1992. *High Resolution Field Gamma Spectrometry and its Application to Problems in Environmental Radiology.* Thesis (PhD). Department of Radiation Physics, Malmö and Lund, Lund University.

Geller, M. and Edward, W., 1969. A table of integrals of the exponential integral. *Journal of Research of the National Bureau of Standards, Section B: Mathematical Sciences,* 73B (3), 191-210.

Huddleston, C. M., Klingler, Q. G., Burson, Z. G.and Kinkaid, R. M., 1965. Ground Roughness Effects on the Energy and Angular Distribution of Gamma Radiation from Fallout. *Health Physics*, 11 (6), 537-548.

Isaksson, M., 2011. Environmental Dosimetry – Measurements and Calculations. *In:* Singh, N., ed. *Radioisotopes - Applications in Physical Sciences*. Rijeka: InTech, 175-196.

Kock, P., 2012. *Orphan source detection in mobile gamma-ray spectrometry – Improved techniques for background assessment*. Thesis (PhD). Department of Medical Radiation Physics, Malmö, Lund University, Sweden.

Kovalev, E.E. and Foderaro, A., 1968. Surface sources *In:* Jaeger, R.G., ed. *Engineering Compendium on Radiation Shielding. Volume I – Shielding Fundamentals and Methods*. Berlin: Springer-Verlag, 368-369.

Leo, W.R., 1994. Techniques for Nuclear and Particle Physics Experiments: A How-to Approach. 2nd ed. Heidelberg: Springer Verlag, 109-111.

OCDM, 1961. *Design and Review of Structures for Protection From Fallout Gamma Radiation*. OCDM Engineering Manual, Part A. Fort Belvoir, VA., U.S. Army 50 pages.

Spencer, L.V., 1962. *Structure Shielding Against Fallout Radiation From Nuclear Weapons*. National Bureau of Standards Monograph 42. Washington, D.C., U.S. Government Printing Office. 134 pages.

SSM, 2010. *Strålsäkerhetsmyndighetens föreskrifter om hantering av radioaktivt avfall och utsläpp från verksamhet med öppna strålkällor*. SSMFS 2010:2. Stockholm, Swedish Radiation Safety Authority.